UNIVERSITY OF TARTU

Faculty of Science and Technology

Institute of Chemistry

Inga Põldsalu

An AFM study of reactive sputter-deposited oxide films used as solid support for lipid nanotubes networks

Master's thesis

Supervisors:

PhD student Irep Gözen

Dr. Urmas Johanson

Associate professor Uno Mäeorg

Tartu 2012

Table of Contents

1 Introduction

Phospholipid films closely resemble cell membranes in structure and composition and therefore serve as model systems in investigations of transmembrane transport, membrane protein function, drug-receptor interactions, and others. Biomembrane based applications, such as sensors or surface-based separation devices often require boundaries formed by lipid membranes [1].

In order to improve stability and usability, surface-adsorbed phospholipid films, often referred to as solid-supported bilayers, have been developed. They are commonly utilized as biomimetic substrates. For example, the integration of membrane proteins as functional components is now a major application area of supported bilayers, covering sensing technology, drug delivery, chemical and cell biology, biomedicine and others[2–4].

The nature of the solid support is of fundamental importance for the type of lipid film formed on its surface. High energy surfaces, such as silicon oxide, aluminium oxide or titanium oxide, are known to support lipid bilayers, where the lipid head groups interact with the surface. In contrast, monomolecular films are formed exclusively on polymer surfaces, where the lipid tail groups face the hydrophobic surface and screen the aqueous environment.

In this thesis, aluminium oxide, titanium dioxide and silicon dioxide surfaces were produced by reactive sputtering of aluminium, titanium and silicon targets in an oxygen atmosphere, and the resulting oxide films were characterized by atomic force microscopy (AFM), and subsequently used to investigate the formation of dense lipid nanotube networks by tension-driven transformation of solid supported bilayers. Highly branched lipid nanotube networks are commonly found in the endoplasmic reticulum and the Golgi apparatus. A solid-supported model system for the ER and Golgi networks can help to improve our understanding of intracellular materials transport. To establish a relationship between surface topology and lipid film properties was the main aim of this thesis.

2 Literature overview

2.1 Substrates

The most common surfaces used for lipid bilayer adhesion for research purposes are optically transparent (quartz, mica, soda-lime, borosilicate glass) and therefore compatible with many microscopy and spectroscopy applications. Silicon dioxide and titanium dioxide are high-energy surfaces which can be deposited onto solid substrates in thin transparent layers.[5]

Very important thing in fabricating these thin films is cleanliness. Glass cover slips that are being worked with must be cleaned very thoroughly to remove all the organic and inorganic particles, to avoid the contamination of the film that is being deposited and to guarantee the best adhesion with the substrate. Because of the structure of the lipid membranes that are being investigated thin films that are somewhat hydrophilic are preferred.

Due to the small feature sizes that can be fabricated, larger particles such as dust and droplets must be avoided during the fabrication procedure. This is achieved inside clean room facilities with a maximum allowed particle density according to clean room facility standards, as well as other requirements.

2.1.1 Deposition of thin oxide films

There are several options to deposit thin oxide films, e.g., chemical vapor deposition, atomic layer deposition, thermal evaporation, pulsed laser deposition and sputtering.

Sputtering was chosen for this work, because it has many advantages over other deposition methods.

DC sputtering is a method for the deposition of various materials, electrically conducting or insulating. The process takes place in an evacuated chamber, where a disc-shaped target material is bombarded with a flow of argon ions. The target also serves as a cathode. The argon ions are created in plasma. They interact differently with the target material depending on their energy of impact they receive from plasma. If the energy is between 10 to 5000 eV, surface atoms are removed from the target, which is actual sputtering process shown in Figure 1. A stream of ejected surface atoms away from the target is created, and these atoms condense at the opposing substrate which is placed above an anode. The condensation process at the substrate is called deposition.[6]

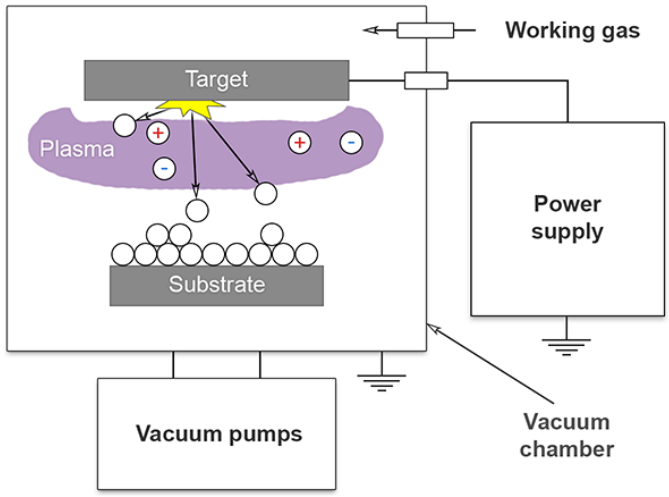

Figure 1. Scheme of the sputtering process.

In RF sputtering there is no direct current between anode and cathode, but the current alternates at high radio frequencies (RF). It is mostly used to sputter insulators and require high bias for the sputtering process to occur. By using an alternative current, a build-up of charges at the target and at the substrate is prevented. Common examples of an RF sputtered material are different metals, where in the presence of oxygen in the sputter chamber, films of metal oxide are deposited. In this process called Reactive Sputter Deposition, atoms of the ambient gas in the chamber react with surface atoms and are built into the film. Additionally a magnetron can be used in DC or RF sputtering in order to yield maximal sputter rates at lower argon pressure and to minimize substrate heating.[7]

An important advantage of sputter deposition is that even materials with very high melting points are easily sputtered, while evaporation of these materials in by evaporation is problematic or impossible. Sputter deposited films have a composition close to that of the source material. The difference is due to different elements spreading differently because of their different mass (light elements are deflected more easily by the gas) but this difference is constant. Sputtered films typically have a better adhesion on the substrate than evaporated films. A target contains a large amount of material and is maintenance free making the technique suited for ultrahigh vacuum applications. Sputtering sources contain no hot parts (to avoid heating they are typically water cooled) and are thus compatible with reactive gases such as oxygen. It is also a fast technique and provides good thickness control. Formed film surfaces are typically smooth and they can therefore be analyzed with atomic force microscopy (AFM).

2.1.2 Scanning Probe Microscopy methods

Scanning probe microscopy (SPM) is a widely used technique for characterizing materials' surfaces down to the atomic scale. Depending on measuring method, SPM allows to investigate large variety of materials. It is possible to carry out SPM experiments in very different environments – in ultra high vacuum, controlled gas environment, ambient conditions and in liquids.[8]

In SPM techniques the sharp probe is either scanned across a sample or the surface is scanned beneath the probe. Interactions between the tip and the sample are detected and mapped. Different techniques sense different interactions, which can be used to describe surface topology, adhesion, elasticity, conductivity, etc.

AFM is one of the main imaging methods of SPM.

The AFM method was first introduced in 1986 by Binning *et al.*, and provided a vertical resolution of 0.1 nm and lateral resolution of 3 nm.[9] The constraint of the resolution limit of optical microscopy these days could thus be overcome with AFM.[7] It can image features as small as an atomic lattice, for either conductive or non-conductive samples. The technique makes it possible to image the samples in-situ, in fluid, under controlled environments. AFM imaging relies on a small AFM probe that is raster scanned over a surface to generate an image. The probes have two major components; a flexible cantilever, which is attached to the probe chip, and a sharp probe tip near the end of the cantilever. AFM probes can be manufactured from a variety of materials, but are mostly made of silicon and/or silicon

nitride. The tip diameter can vary, depending on its specific application, but it is generally extremely sharp, usually on the order of a few nanometers to tens of nanometers in radius at the tip apex. Various novel techniques have been developed for creating even sharper tips, for example, carbon nanotubes and tungsten nanowires have been added to the end of the probes[5], [10]. The potential of AFM extends to applications in life science, material science, electrochemistry, polymer science, nanotechnology, biotechnology, etc.[11], [12]

Contact mode and dynamic mode are two major AFM imaging modes.

2.1.2.1 Contact mode AFM

In contact mode, the AFM probe tip is in continuous contact with the sample, where the tip is deflected when it approaches the surface. The deflection of the tip is measured with a laser that is reflected from the cantilever's top surface onto a photodiode. Typically, the forces applied to samples in CM are in the range from tens to hundreds of nano-Newtons (nN).[8] A drawback of the contact mode is the possibility that the tip gets contaminated by the sample. Insulating or semiconductor samples can additionally build up charges which distort the image. In ambient conditions, most samples develop a liquid meniscus layer. Keeping the probe tip close enough to the sample for short-range forces to become detectable, while preventing the tip from sticking to the surface, presents a major problem for non-contact dynamic mode in ambient conditions.[13] In order to solve these problems, AFM can be used in dynamic mode.[7]

2.1.2.2 Dynamic mode AFM

In contrast to contact mode, in dynamic mode the AFM probe is oscillated at high frequencies above the sample. One advantage of this mode is that the probe does not contact at all or contacts very slightly and/or shortly with the sample surface.[8]

There are two main dynamic mode imaging techniques – non-contact mode and tapping mode.

A stiff cantilever is oscillated in the attractive regime, meaning that the tip is quite close to the sample, but not touching it (therefore, "noncontact"). The forces between the tip and sample are quite low, on the order of pN (10^{-12} N). The detection scheme is based on measuring changes to the resonant frequency or amplitude of the cantilever.[14]

In tapping mode a stiff cantilever is oscillated closer to the sample than in noncontact mode. Part of the oscillation extends into the repulsive regime, so the tip intermittently touches or

“taps” the surface. Very stiff cantilevers are typically used, as tips can get “stuck” in the water contamination layer.[14]

This method of "tapping" lessens the damage done to the surface and to the tip compared to the amount done in contact mode.[15]

2.2 Phospholipid membranes

2.2.1 Lipids and lipid bilayers

Lipids are amphiphilic, consisting of both hydrophilic and hydrophobic parts. In water amphiphilic molecules may self-assemble into aggregates, such as micelles and bilayers. Vesicles made of lipid bilayers (i.e. liposomes) are often used as a model for studying properties of cell membranes.

A biological membrane or biomembrane is an enclosing or separating membrane that acts as a selective barrier, within or around a cell.[16] The plasma membrane encloses the interior of the cell and separates it from the surrounding medium as well as from other cells. Inside the cell special compartments (such as the endoplasmatic reticulum, Golgi complex and mitochondria) are enclosed by membrane. Various biological membranes have different composition and functions, but they all possess a common general structure - every membrane is a very thin film consisting of lipids and proteins. Most animal cell membranes consist of about 50% of lipid molecules and nearly all the rest belongs to proteins.[17]

Lipid molecules have a hydrophobic head group and one or two hydrophobic tails. In water the hydrophilic part of the molecule is attracted to the water. The hydrophobic part tries to avoid water by sticking together with other hydrophobic molecules and because of that aggregates form. The different shapes of the lipid molecules give different types of aggregates, which are characterized by a shape factor $v/a_0 l_c$, where a_0 is the interface area occupied by the polar head group, and v and l_c are the volume and length of the hydrocarbon region. The value of the shape factor determines whether lipids form: micelles ($v/a_0 l_c < 1/3$) shown in Figure 2; non-spherical (globular or cylindrical) micelles ($1/3 < v/a_0 l_c < 1/2$); bilayers ($1/2 < v/a_0 l_c < 1$) shown in Figure 3; or inverted micelles also known as vesicles ($v/a_0 l_c > 1$)[18] illustrated in Figure 4. In particular, cylindrical micelles are composed of single-chained lipids with small head group areas, while bilayers are formed by double-chained lipids with large head group areas.

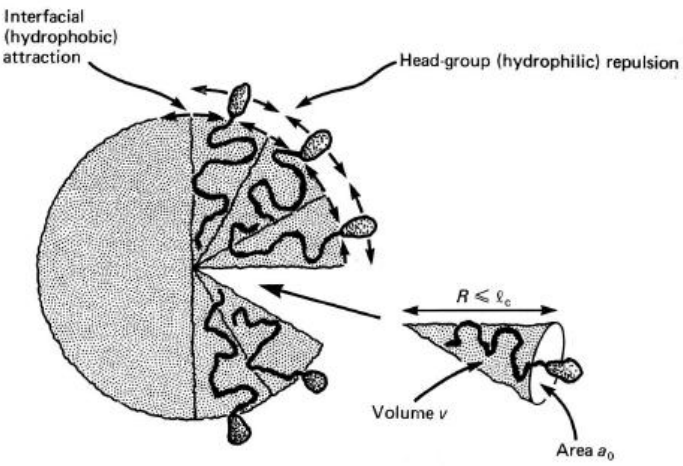

Figure 2. In case of a small shape factor lipids form micelles.[40]

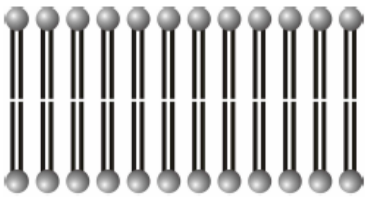

Figure 3. When the shape factor is between 1/2 and 1 lipids form bilayers.[40]

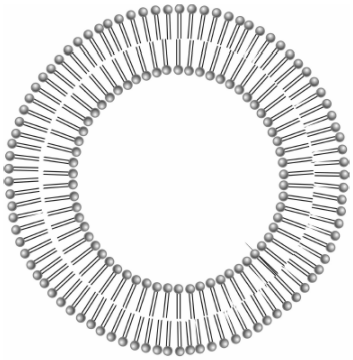

Figure 4. When the shape factor is bigger than 1 lipids form vesicles.[40]

The most common biological membrane lipids are the phospholipids.

Phospholipids head group is linked to two hydrophobic hydrocarbon tails through a phosphate group. In most biological membranes, hydrocarbon tails contain from 10 to 18 carbons per chain, one of which is unsaturated or branched. Due to their cylindrical shape and amphiphilic nature, phospholipids can spontaneously form membranes, which provide one of the main properties of cell membrane: to be impermeable for ions and polar molecules[17]. Closed

spherical compartments, or liposomes, are special form of phospholipid bilayer membranes, where a part of the external aqueous medium is encapsulated.

Liposomes are often classified according to their size and number of bilayers in a vesicle. If a vesicle consists of a single bilayer then it is called a unilamellar vesicle. Vesicles that have more than one bilayer are referred to as multilamellar. Based on their size they are classified as small (10-50 nm), large (50-1000 nm) and giant vesicles (larger than 1 μm). Giant unilamellar vesicles (GUVs) are easy to observe by using light microscopy because of their size. Flat giant unilamellar vesicles (FGUVs), which can essentially be viewed as intact double bilayer phospholipid films, are formed by spreading of multilamellar (onion shell) vesicles on solid supports. In the present work, a method originally developed by Criado and Keller[19] with some modifications[20] is used to prepare the needed multilamellar vesicles.

Supported lipid bilayers can be assembled on many types of high energy surfaces, such as metals, metal oxides, semiconductor oxides and nitrides[5]. These surfaces are usually hydrophilic and have somewhat negative zeta potential, similar to most phospholipid assemblies that contain phosphatidylserine (PS), phosphatic acid (PA) and phosphatidylinositol (PI) (which are more commonly used phospholipids for membrane preparations).

Lipid bilayer formation is also strongly dependant on the buffer composition[21]. Buffers with high ionic strength will aid lipid bilayer formation due to multivalent cations, which screen the negative charges of substrate and lipids. Calcium (Ca^{2+}) and magnesium ions (Mg^{2+}) have been shown to bind to negatively charged lipid bilayers. Ca^{2+} is most commonly used to electrostatically bridge between the negatively charged substrate and the lipid bilayer, thereby promoting adhesion.[5] Initially these ions were used to were found to promote fusion of lipid vesicles, and are therefore often referred to as ‘‘fusogenic agents’’.[22] On positively charged corundum (Al_2O_3) surfaces,[23] as well as on SiO_2 chemically modified with positively charged 3-aminopropyldimethylethoxysilane,[24] phospholipid vesicle adsorption and rupture is promoted even in the absence of fusogenic agents. This is due to the strongly attractive charge interaction. Tero et al. have studied phospholipidvesicle adsorption on SiO_2 with controlled hydrophilicity, and thus, surface energy.[25] Chinese hamster ovary (CHO) cells were found to spread on SiO_2, eventually leading to plasma membrane rupture when europium ions (Eu3+) were present in solution.[26]

Substrate smoothness plays an important role in lipid bilayer spreading.[27] The rougher a substrate, the more bending energy of the lipid bilayer needs to be stored in the system, which is balanced with the energy gain upon bilayer wetting.

2.3 Self spreading of multilamellar vesicles

Deposition of lipid reservoirs on high-energy surfaces in aqueous environments leads to the formation of self-spreading surface-supported lipid bilayers. Lipid reservoirs range from manually deposited single bulk lipid sources (multilamellar or onion-shell liposomes)[5][29] to aqueous vesicle suspensions of different particle sizes, which can be directly pipetted onto the substrate. In the former case, a single continuous lipid film is spreading from a lipid source, whereas in the latter case, small lipid films originating from each single surface-adhered vesicle coalesce into contiguous patches eventually forming a continuous film.

Reimhult et al. found that vesicle rupture occurs either immediately when the particles come into contact with the substrate or, alternatively, after a critical concentration of surface adhered vesicles is reached.[30] Upon rupture, bilayers are folding back onto the surface.[31] Electrostatic interactions are of vital importance for this process to occur.

Dimitrievski and Kasemo provided a model for vesicle rupture that considered lipid composition and surface charge density to be key parameters.[32] A recent article by Gromelski et al. reviews lipid bilayer formation specifically under the aspect of surface and lipid properties.[33]

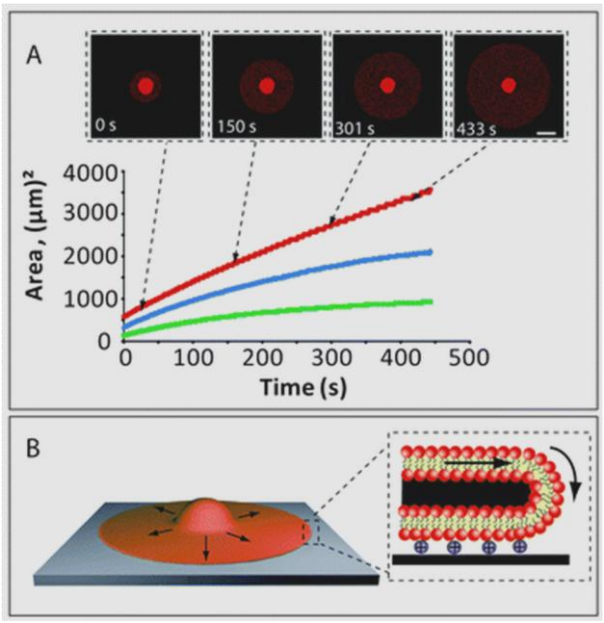

Figure 5. The graph shows the area increase in the surface-adhered membrane with time in three different experiments. The initial radii of the vesicles were 13.6, 10.3, and 6.6 µm, respectively. Confocal microscopy images (inset) show the circular membrane spreading in one of the experiments. Scale bar 20 µm. (B) Schematic drawing showing juxtaposed lipid bilayer spreading from a multilamellar vesicle in a circular manner. The inset shows the advancing edge of a vesicle.[21]

Tank-thread-like rolling of stacked bilayers has been identified as another spreading mechanism (Figure 5). In this case, vesicle integrity is maintained and the internal content is preserved. It is currently unclear how much the distal and the proximal bilayer contribute to the spreading process. Double bilayer spreading was observed when the cholesterol contents

of the bilayer exceeded 45 %.[34] Also, it occurs to a varying degree depending on the ionic strength,[35] which was confirmed by the findings of Gözen et al.[26]

Gözen et al. observed two different rupture mechanisms in bilayer membranes spreading on solid supports: in one case rupture resulted in floral like pores (Figure 6 IV where pore is growing and V, complete layout of the film) and in the other one rupture proceeded in a series of rapid avalanches causing fractal membrane fragmentation (Figure 6 IV' and V').

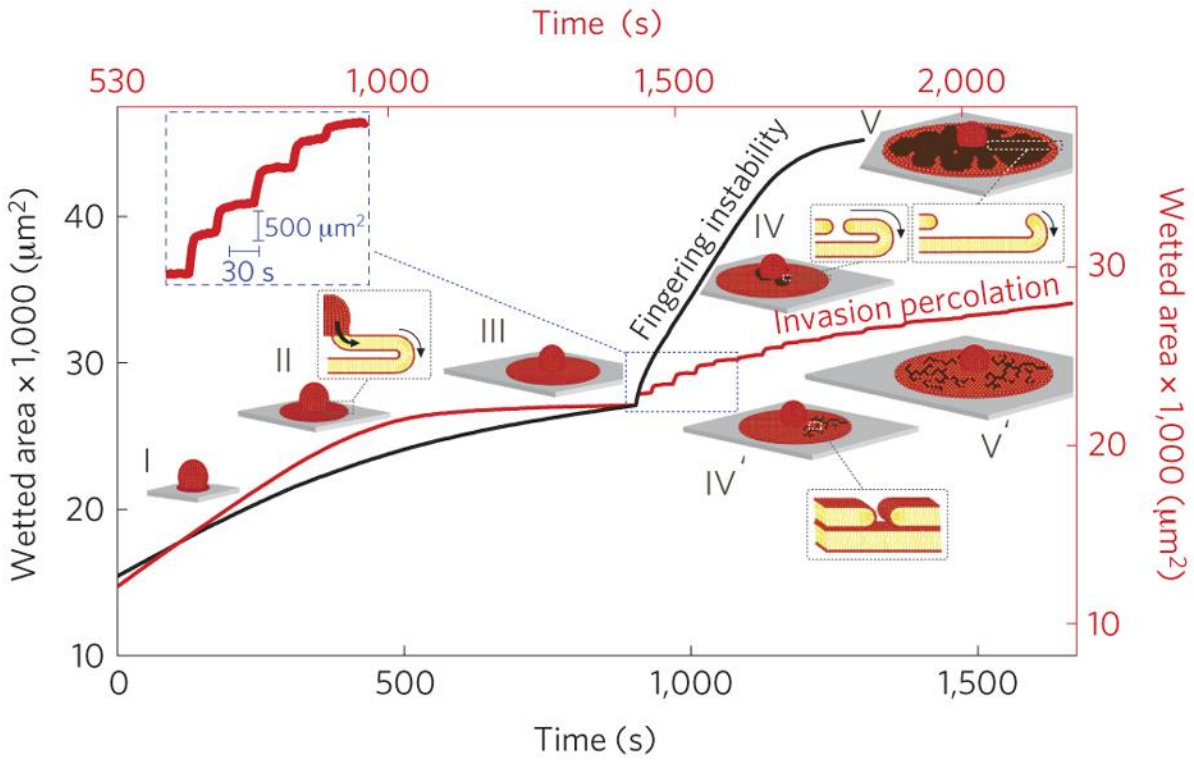

Figure 6. Increase in wetted surface area in growing flat unilamellar vesicles undergoing floral and fractal membrane rupture.[26]

Gözen et al. also found a procedure to reverse the pore formation by chelating the Ca^{2+} ions, which stabilizes the pores and makes them close.[36]

In the process of trying to find a way to have a persisting avalanche ruptures (it is yet unknown which way the rupturing goes) and working with the closing of the pores, new kind of lipid behavior was discovered. When changing the surface of the glass cover slip then after the spreading and chelating of the Ca^{2+} ions is done, tubulation appears, shown in the Figure 7. After a while the MLV starts spreading again and ULV spreads between the tubes (shown in the Figure 8).

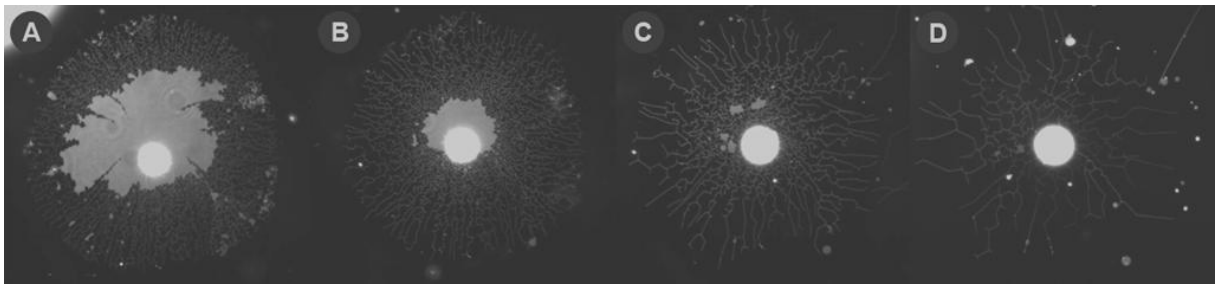

Figure 7. Forming of the tubes on 10 nm thick Al_2O_3 film. A and B show the different stages of the tubulation process, on C and D it is shown that the material in the tubes goes back into the MLV.

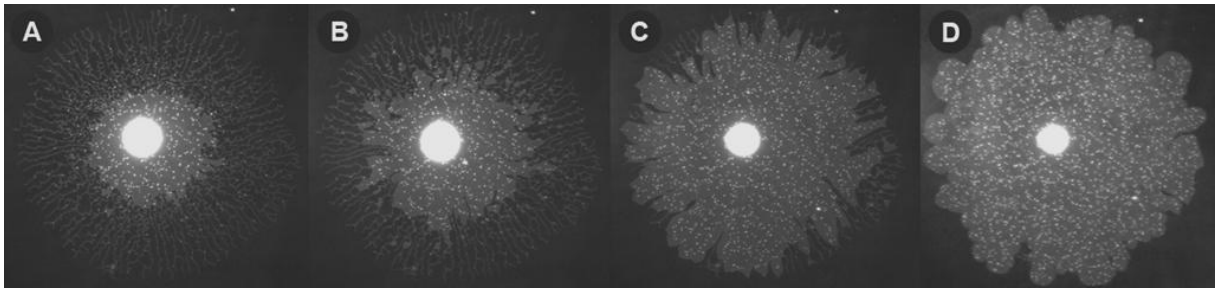

Figure 8. Spontaneous process where vesicle spreads between the lipid tubes.

2.4 Imaging methods for lipid structures

Analytical methods based on optical principles, mainly using light from within the visible and infrared range, are commonly applied to investigate supported lipid films. Te thickness of a bilayer membrane of ~4 nm is well below the diffraction limit of light microscopy, meaning that direct observation is not possible. Common optical fluorescence based methods such as laser induced fluorescence and confocal fluorescence are therefore used to study supported phospholipid films.[1]

2.4.1 Fluorescence microscopy

Fluorescence microscopy requires staining of the specimen with fluorescent molecules, or dyes. Fluorescent molecules absorb light in one wavelength band and emit light at longer wavelengths. When fluorescent molecules absorb light in excitation wavelength, they are excited to a higher electronic state. This state has a short lifetime and the molecules will release the energy in the form of light and heat. Since some energy is dissipated as heat, the emission light contains less energy and therefore has a longer wavelength than the absorbed excitation light. This emission of light is referred to as fluorescence. Introducing several fluorescent dyes with different emission wavelengths gives the possibility to study several molecules species simultaneously. In the present work, the Laser Induced Fluorescence technique is used, which means that laser light is used to induce fluorescence.[26][37]

Inside the microscope, an objective plays a key role: it focuses the laser light into a small spot onto a specimen and then also collects the fluorescence light and images it into the detector. Objectives also determine the magnification of a particular specimen and the resolution under which fine specimen detail can be observed in the microscope. The resolution can be defined as the smallest distance between two points on a specimen that can still be distinguished as to separate entities. The objective resolution (OR) depends on the wavelength (λ) of light used to image a specimen, and the numerical aperture (NA) of the objective: $OR = 0.61\frac{\lambda}{NA}$. The numerical aperture is also one of the important parameters of an objective, which describes how good an objective is in collecting light. The numerical value is given by $NA = n \cdot \sin\theta$, where n is the reflective index of the medium and θ is the semi-aperture angle, which is half of the angle of the maximum cone of light that can enter the objective. A higher numerical aperture provides better resolution of the objective.

2.4.2 Confocal fluorescence Microscopy

The term confocal fluorescence microscopy (CFM) is normally used when describing a microscopic technique that provides 3D optical resolution. 3D resolution is accomplished by suppressing a signal coming from out-of-focus plane by introducing a pin-hole in front of the detector. Light originating from an in-focus plane is imaged by the microscope objective in such a way that it passes a pin-hole, while light coming from out-of-focus is largely blocked by a pin-hole. In conventional fluorescence microscopy, both signals coming from the focal plane and out of focus are collected, which causes blurring of the image.[38]

Another advantage of CFM is that the laser beam is highly focused so that the illumination density drops off rapidly above and below the plane of focus. A combination of advanced detectors and illumination techniques, together with modern software packages and high-performance computers, makes CFM a powerful tool for imaging cellular compartments and even detecting single molecules.[39] The disadvantage of this method is relatively low resolution, which does not allow monitoring fast events.

3 Experimental work

3.1 Materials and methods

3.1.1 Surface fabrication

Glass cover slips (Menzel Gläser) were cleaned using wetbench (Wetbench, Stangl). First they were sonicated in presence of Microposit remover 1165 (Shipley), then rinsed 2 minutes in filtered 2-Propanol bath and lastly flushed 3 minutes in quick damp rinse tank. Glass was dried with N_2 blowgun. After drying, it was oxygen plasma treated at 50 W for 2 minutes in Plasma etch (Plasma Therm BatchTop PE/RIE m/95). Metal oxide was deposited onto the cleaned glass substrate by reactive sputtering, using a MS 150 Sputter system (FHR Anlagenbau GmbH) shown in Figure 9. Three different oxides were deposited: Al_2O_3, SiO_2 and TiO_2, each with two different film thicknesses - 10 nm and 84 nm.

All steps of fabrication were performed in clean room facility MC2, at Chalmers University of Technology in the Process Lab 1 with a cleanroom class 3-6 according to ISO standard 14644-1.

Figure 9. Used sputter system in cleanroom.

3.1.2 Imaging

Optical Microscope

An inverted microscope (Leica DM IRB, Wetzlar, Germany, equipped with a Leica PL Fluotar 10x/0.30 PH 1 objective, was used for imaging. Texas Red DHPE was excited at 532 nm by a green solid state laser MGL-III-532 (Changchun New Industries, Changchun, China). A Chameleon USB camera (Point Gray Research Inc., Richmond, Canada) was used with Fly Capture SDK software to collect the images. Time series were recorded with 2 frames/min sampling frequency.

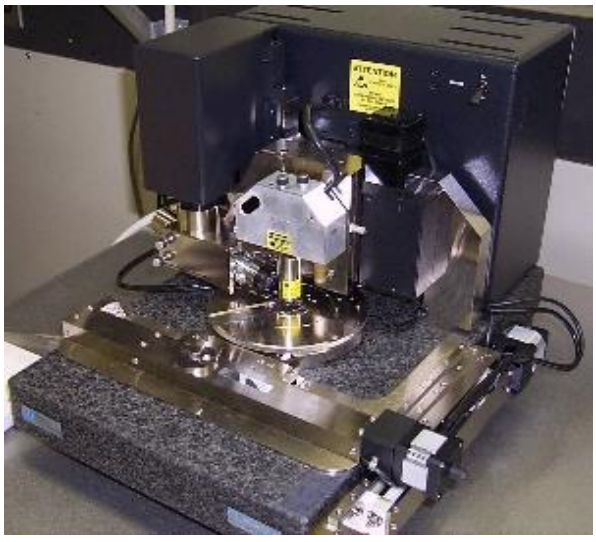

Figure 10. AFM used for imaging

Atomic force microscopy

To reveal the oxide film surface structure in more detail, scanning probe microscopy

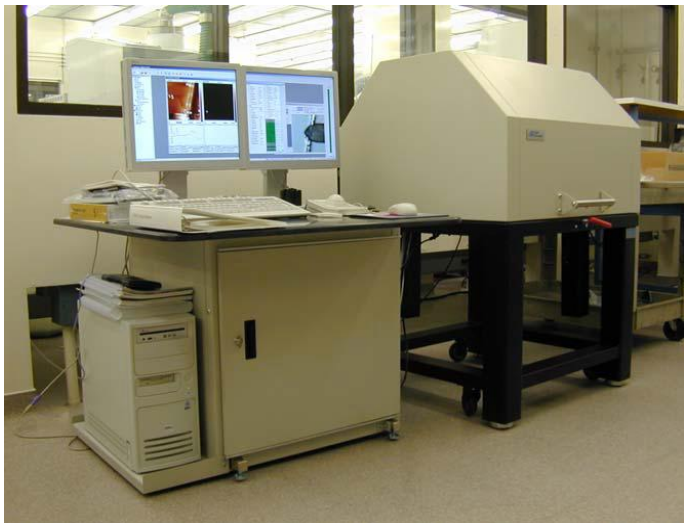

Figure 11. AFM is located inside the hood next to the computer.

(SPM) (Veeco Dimension 3100 ICON SPM) was used (Figure 10). The scanning was performed in tapping mode using different probes (brought out in Table 1.) SPM was positioned in clean room facility MC2 at Chalmers University of Technology in the Process Lab 2 with a cleanroom class 7-8 shown in Figure 11. Describing the surface of the oxide films was done with a program Nanoscope 8.10 and they were processed with a program Nanoscope Analysis 1.20.

3.1.3 Vesicle preparation

To make multilamellar lipid vesicles, a dehydration/rehydration technique [19] was used with modifications [20] to prepare the liposome suspension (10 mg/ml) containing Phosphatidyl choline (69 % w/w) and Phosphatidyl inositol (30 % w/w) and Texas Red full name TR-DHPE (1% w/w).

Both lipids were obtained from Avanti Polar Lipids (Alabama, USA). 3 µl of this suspension was dehydrated on a cover slip for 20 minutes in an evacuated desiccator. Dried lipid film was subsequently rehydrated with 1 ml of 10 mM HEPES (4-(2-hydroxyethyl)-1-piperazineethanesulfonic acid) buffer (10 mM HEPES, 100 mM NaCl, pH adjusted to 7.8 with NaOH solution) to allow the formation of multilamellar vesicles (MLVs). 10 mM HEPES buffer with 4 mM Ca^{2+} was used in the observation chamber for the spreading of MLVs. 10 mM HEPES buffer containing 10 mM EDTA (Ethylenediaminetetraacetic acid) and 7 mM BAPTA (1,2-bis(o-aminophenoxy)ethane-N,N,N',N'-tetraacetic acid) was used to induce the tubular network formation. MLV samples were transferred into an observation chamber, the substrate with metal oxide film at the bottom, containing 5 ml of 10 mM HEPES buffer with 4 mM $CaCl_2$. After MLVs spread and ruptures appeared, the buffer solution containing 10 mM HEPES, 100 mM NaCl, 10 mM EDTA and 7 mM BAPTA (pH=7.8 adjusted with NaOH) was slowly injected into the observation chamber via an automatic pipette while the same means the ambient buffer containing 4 mM Ca^{2+} was removed.

Deionised water Milli-Q system (Millipore) was used for cleaning and preparation of all solutions.

4 Results and discussion

4.1 Preparation of oxide films

Glass cover slips were cleaned successfully in the cleanroom environment with chemical compounds as well as with oxygen plasma. After cleaning process four oxide films were deposited with reactive sputtering: 10 nm of Al_2O_3, 84 nm of Al_2O_3, 84 nm of SiO_2 and 84 nm of TiO_2.

4.2 Characterization of oxide films

Deposited oxide films were characterized with AFM, which was used in tapping mode. Probes used in this work are shown in Table 1.

Probe	Tip material	Company	Probe tip radius (nm)	Probe tip angle °	Problems
NSC15	Si	Mikromasch	10	40 °	Charge effects
NSC15 Ti-Pt	Si with Ti-Pt coating	Micromasch	40	40 °	Charge effects
NSG10 TiN	Si with TiN coating	K-Tek Nanotechnology	10	40 °	Low resolution
TESPA	Si	Bruker	8	40 °	Low resolution
Hi'RES-W	Si with W-spike	Micromasch	1		-

Tabel 1 Probes used in this work.

Since the topography of the film was unknown, the first probe that was used was NSC15 from Micromasch. The probe is made of phosphorus doped n-type silicon. It has a conical shape with 10 nm tip radius and a 40° full tip cone angle. Imaging with that tip was problematic due to charge effects. To get rid of the charge effects the probe was changed to NSC15 with a Ti-Pt coating. It is the same tip as NSC15, but it has a conductive coating. The Ti-Pt coating consists of a 10-nm Pt layer on a 20-nm Ti sublayer, which increases adhesion and electromigration firmness of Pt. Due to the coating the tip radius is four times bigger. That probe also did not give good results, because of the wearing of the conductive layer which leads to charge effects. The imaging was then continued with a NSG10 TiN probe which is

made of antimony doped n-type single crystal silicon that is coated with TiN. TiN is an extremely hard ceramic material. Its thin layer is used to harden and protect softer materials.

With the TiN probe the charge effects were eliminated, but there appeared to be another problem, the resolution was too low for these films. Next the Tespa probe was tested, it has somewhat smaller tip radius, but the charging effects appeared again. The last probe that was used was Hi'Res-W probe. It is a silicon tip with a single tungsten spike at the end. It provides high resolution and has a minimum tip-sample attraction force. When imaging the surface it gave no problems and it was used to scan all the AFM-images shown in this work.

4.3 AFM scans

Having a problematic (broken, contaminated, etc.) probe may lead to incorrect images that have artifacts as the one shown in Figure 12.

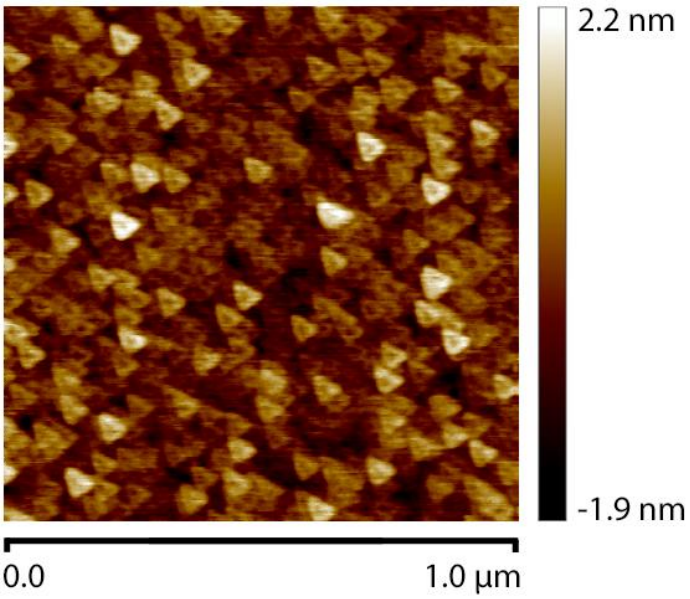

Figure 12 Image recorded with a contaminated tip.

When scanning the Hi'Res-W probe along the surface, good quality images were recorded of the topography of the oxide films such as 10 nm thick Al_2O_3 in the Figure 13, 84 nm thick Al_2O_3 in the Figure 14, 84 nm thick SiO_2 in the Figure 15 and 84 nm thick TiO_2 in the Figure 16.

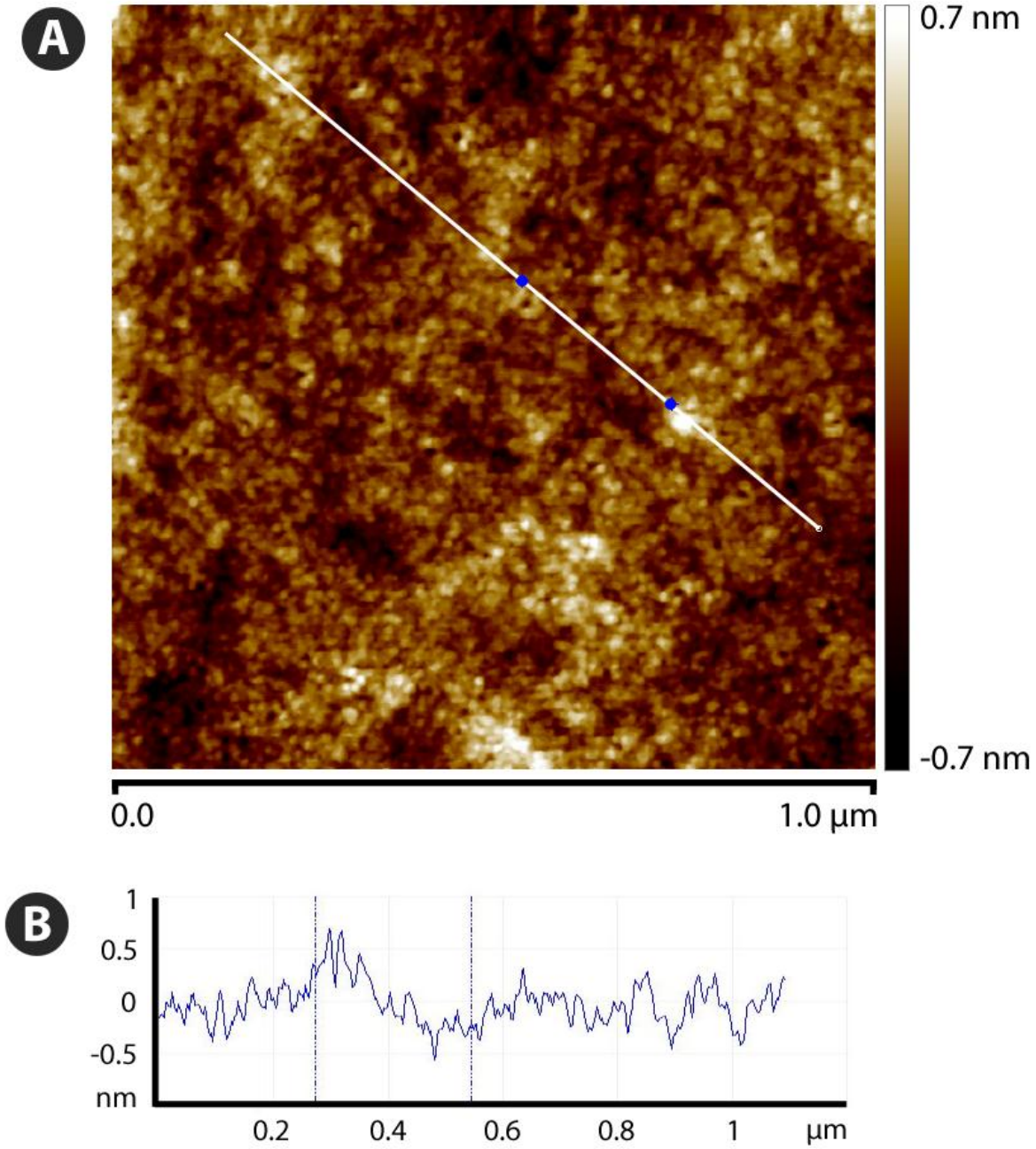

Figure 13. **A)** AFM image of 10 nm thick Al_2O_3 surface. Image has been flattened. **B)** Topography profile along the white line.

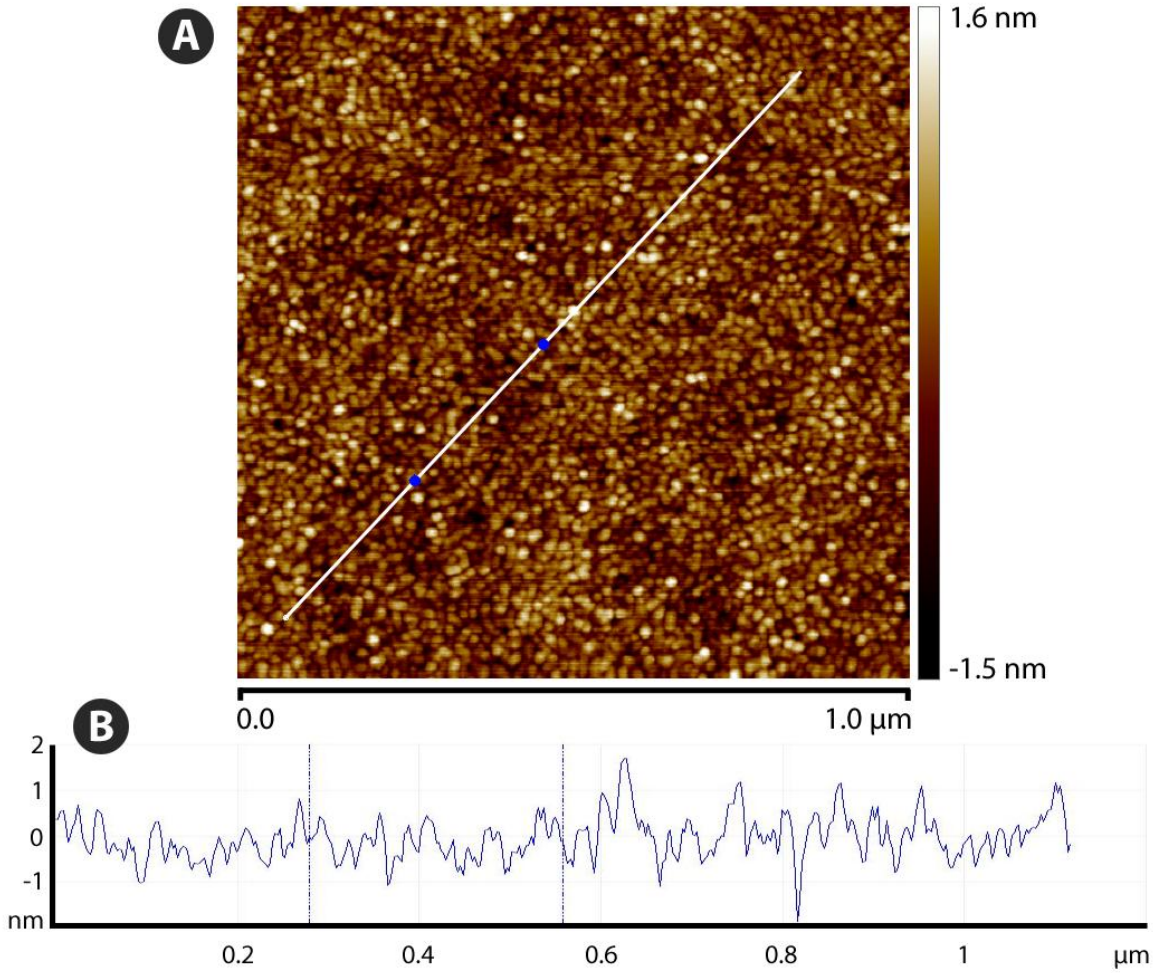

Figure 14. **A)** AFM image of 84 nm thick Al_2O_3 surface. Image has been flattened. **B)** Topography profile along the white line.

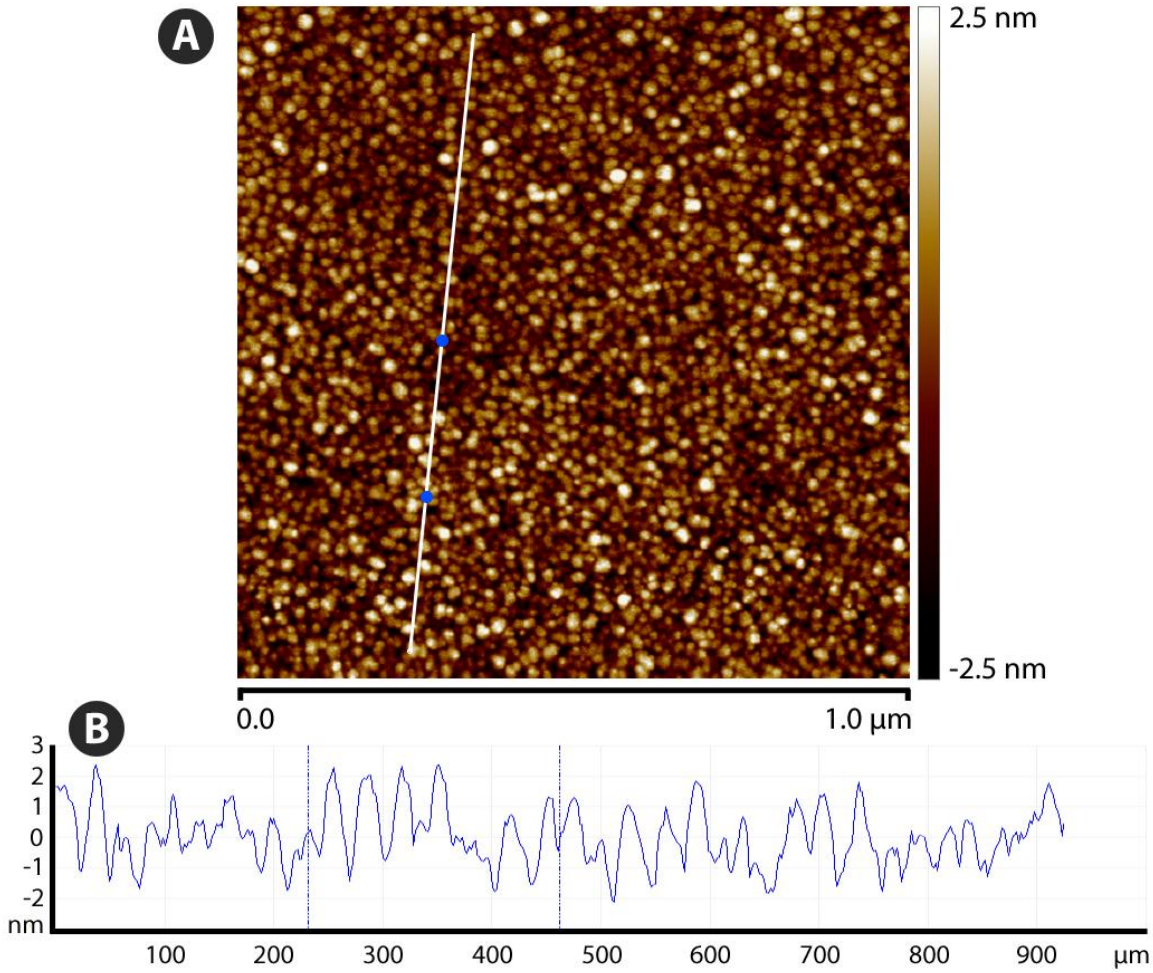

Figure 15. **A)** AFM image of 84 nm thick SiO_2 surface with. Image has been flattened. **B)** Topography profile along the white line.

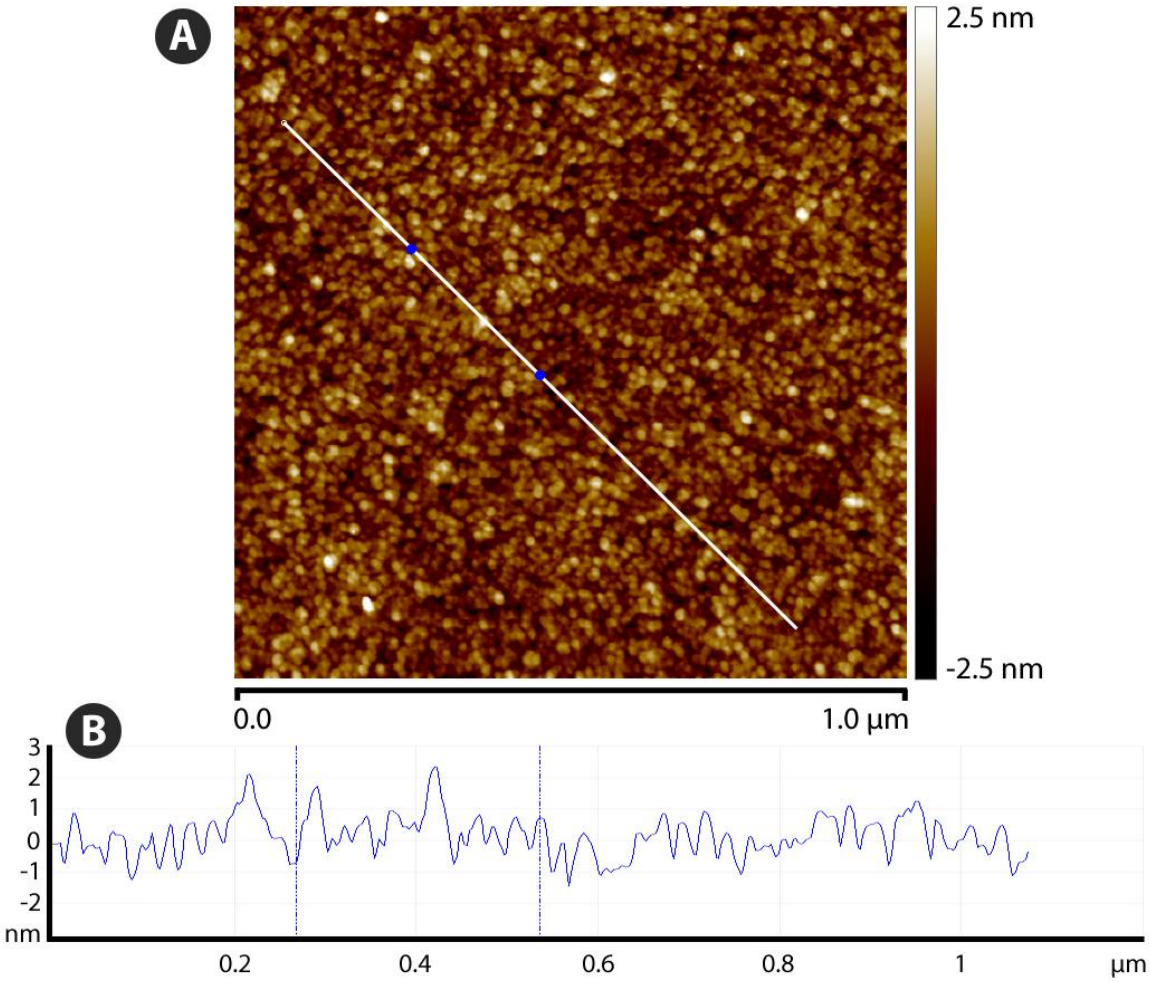

Figure 16. **A)** AFM image of 10 nm thick Al_2O_3 surface **B)** with topography profile along the white line. Image has been flattened and 3x3 median filtered.

In the Table 2 the thickness of the oxide films is shown, as well as their RMS roughness and z-range.

Material of the film	Thickness of the film (nm)	RMS roughness (nm)	Z-range (nm)
Al_2O_3	10	0.20	2.06
Al_2O_3	84	0.44	4.82
SiO_2	84	0.86	8.17
TiO_2	84	0.62	6.09

Tabel 2 Deposited and analyzed films

The AFM characterization of the oxide films shows that the films are really smooth with the z-range variation from 2 nm to 8 nm. Z-range is in correlation with the RMS roughness in the experiments done in this work. The root mean square (RMS) roughness of 84 nm thick Al_2O_3

film is double of the 10 nm thin Al_2O_3 RMS rougness. SiO_2 with 6 nm of z-range and 0.6 nm of RMS roughness is the roughest film of the four.

4.4 Occurring lipid tubulation processes on oxide films

After depositing oxide films on the thoroughly cleaned glass cover slips, the control experiments with the lipids were performed.

It appears, that the smoother the oxide surface, the faster the tubulation process. On the 84 nm SiO_2, that is the roughest examined film, there is no tubulation. The vesicle ruptures almost instantly when deposited onto the surface and after chelating the Ca^{2+} ions, the pore starts to close.

On the 10 nm thick Al_2O_3 film lipid spreads really fast and nicely and after the exchange of the buffer solution, which has the chelating agent, the tubes start to form, the process lasts approximately two hours. After tubulation process slows down, it stays like that for a while and then the multilamellar vesicle starts to spread in between the tubes spontaneously.

The process works only with the type of lipid mixture described in the experiments part. PC-PI-PE mixture is tried in the same experimental setup, but no tubulation is taking place.

5 Summary

The object of this study was to prepare thin oxide films by reactive sputtering deposition in order to use them as solid support for lipid nanotube networks. Formed oxide film surface structure was characterized with AFM, to better understand the lipid film processes taking place on them.

In the first part of the work, the literature of the field of study was perused. In the literature overview all the fabrication methods and research techniques used in this study are covered.

At first, cleaning of the glass cover slips with chemical substrates and plasma are described.

Then the method for depositing the oxide film is described. The structure of the deposited oxide film topography plays an important role in the following processes; therefore, an accurate description of the substrates characterization is very important. In this work, the topography was characterized with AFM. In the literature overview, different SPM methods are described.

In the last part of the literature overview, different lipid structures and their processes are described.

In the experimental part of the work, the exact cleaning process of the glass cover slip and the fabrication method of the thin oxide films are illustrated. The equipment used in the work is introduced, as well as an exact overview of the preparation of the vesicles.

In the results and discussion section, all the important results obtained with AFM are presented. The problems with the unsuitable probes are discussed. The good quality AFM images are characterized with the RMS roughness and with the difference of the lowest and the highest peak.

The preliminary experiments of the lipid structures were made, which are being carried on with the other members of the group. The aim of the work was accomplished and good quality AFM scans of the oxide films topography was obtained. These results are going to be published in an international journal.

6 Kokkuvõte

Lipiidsete nanotoruvõrgustike uurimiseks kasutatavate reaktiivse magnetron-tolmustamise abil sadestatud oksiidsete kilede iseloomustamine AFM-i abil.

Käesoleva töö eesmärgiks oli valmistada oksiidseid kilesid reaktiivse magnetron-tolmustamise abil, selleks et uurida nende pinnal lipiidsete nanotoruvõrgustikega seotud protsesse. Valmistatud oksiidsete kilede pinda iseoloomustati aatomjõu mikroskoobiga (AFM-iga).

Töö esimeses osas on esitatud kirjanduse ülevaade, milles käsitletakse kõiki antud uurimistööga seonduvaid valmistamismetoodikaid ja uurimismeetodeid. Alustuseks kirjeldatakse mikroskoobiklaaside puhastamist keemiliste reaktiivide ja plasma abil.

Järgnevalt kirjeldatakse oksiidsete kilede valmistamisel kasutatud metoodikat. Selliselt valmistatud kilede pinnastruktuur omab olulist tähtsust järgnevate protsesside kulgemisel, mistõttu on selliste aluste täpne iseloomsutamine väga oluline. Selle töö raames kirjeldati pinna topograafiat AFM-i abil. Kirjanduse ülevaate osas tutvustatakse lühidalt erinevaid skaneeriva teravikmikroskoopia (STM) meetodeid.

Kirjanduse ülevaate viimases osas tutvustatakse erinevaid lipiidseid struktuure ja nendega toimuvaid protsesse. Samuti antakse ülevaade nende protsesside uurimiseks kasutatavatest optilise mikroskoopia meetoditest.

Töö eksperimentaalses osas kirjeldatakse täpselt aluste puhastamist ja nendele oksiidsete kilede valmistamist. Tutvustatakse uurimistöö käigus kasutatud aparatuuri ja antakse detailne ülevaade vesiikulide valmistamisest.

Töö tulemusi käsitlevas osas tuuakse ära kõik olulised AFM mõõtmistega saadud resultaadid. Kirjeldatakse probleeme, mis tekkisid seoses algselt kasutatud ebasobivate teravikega. Saadud hea kvaliteediga AFM piltide korral kirjeldatakse iseloomustatavate objektide RMS pinnakaredust ja pinna madalaimate ning kõrgeimate punktide kõrguste erinevust.

Lipiidsete struktuuride uurimisel tehti esmased katsed, mida jätkasid teised uurimisgrupi liikmed. Töö käigus täideti eesmärk ja saadi kvalitseetsed oksiidsete kilede pinnastruktuuri iseloomustavad mõõtmistulemused. Need tulemused on plaanis publitseerida rahvusvahelises teadusajakirjas.

7 References

[1] I. Gözen and A. Jesorka, “Instrumental methods to characterize molecular phospholipid films on solid supports.,” *Analytical chemistry*, vol. 84, no. 2, pp. 822-38, Jan. 2012.

[2] J.-L. Reymond, “Wiley Encyclopedia of Chemical Biology, Vols. 1-4. By Tadhg P. Begley.,” *ChemBioChem*, vol. 10, no. 9, pp. 411-422, Jun. 2009.

[3] E. Sackmann, “Supported membranes: Scientific and practical applications,” *Science*, vol. 271, no. 5245, pp. 43-48, 1996.

[4] M. K. Domanska, V. Kiessling, A. Stein, D. Fasshauer, and L. K. Tamm, “Single vesicle millisecond fusion kinetics reveals number of SNARE complexes optimal for fast SNARE-mediated membrane fusion.,” *The Journal of biological chemistry*, vol. 284, no. 46, pp. 32158-66, Nov. 2009.

[5] I. Czolkos, A. Jesorka, and O. Orwar, “Molecular phospholipid films on solid supports,” *Soft Matter*, vol. 7, no. 10, p. 4562, 2011.

[6] M. J. Madou, *Fundamentals of Microfabrication: The Science of Miniaturization*. CRC Press LLC, 2002.

[7] I. Czolkos, “Micro- and Nano-Scale Devices for Controlling Two Dimensional Chemistry,” Chalmers Unicersity of Technology, 2009.

[8] M. Marandi, “Electroformation of Polypyrrole Films: In-situ AFM and STM study,” University of Tartu, 2011.

[9] G. Binnig and C. Quate, “Atomic force microscope,” *Physical review letters*, vol. 56, no. 9, 1986.

[10] A. B. H. Tay and J. T. L. Thong, “High-resolution nanowire atomic force microscope probe grown by a field-emission induced process,” *Applied Physics Letters*, vol. 84, no. 25, p. 5207, 2004.

[11] H. Dai, J. H. Hafner, A. G. Rinzler, D. T. Colbert, and R. E. Smalley, “Nanotubes as nanoprobes in scanning probe microscopy,” *Nature*, vol. 384, no. 6605, pp. 147-150, Nov. 1996.

[12] M. E. Greene, C. R. Kinser, D. E. Kramer, L. S. C. Pingree, and M. C. Hersam, “Application of scanning probe microscopy to the characterization and fabrication of hybrid nanomaterials.,” *Microscopy research and technique*, vol. 64, no. 5–6, pp. 415-34, Aug. 2004.

[13] Q. Zhong, D. Inniss, K. Kjoller, and V. B. Elings, “Fractured polymer/silica fiber surface studied by tapping mode atomic force microscopy,” *Surface Science Letters*, vol. 290, no. 1–2, p. L688-L692, Jun. 1993.

[14] I. Nanoscience Instruments, “Atomic Force Microscopy.” [Online]. Available: http://www.nanoscience.com/education/AFM.html. [Accessed: 22-May-2012].

[15] Y. Roiter and S. Minko, “AFM single molecule experiments at the solid-liquid interface: in situ conformation of adsorbed flexible polyelectrolyte chains.,” *Journal of the American Chemical Society*, vol. 127, no. 45, pp. 15688-9, Nov. 2005.

[16] K. R. and P. W. B. Alberts, A. Johnson, J. Lewis, M. Raff, *Molecular Biology of the Cell*, 4th ed. Garland Science, 2004, pp. 583-766.

[17] T. Lobovkina, “Lipid Nanotube Networks: Shape Transitions and Insights into the Dynamics of Self-Organization,” Chalmers University of Technology, 2007.

[18] S. M. and R. G. H. J. N. Israelachvili, “Physical principles of membrane organization,” *Quarterly Reviews of Biophysics*, vol. 13, pp. 121-200, 1980.

[19] M. Criado and B. U. Keller, “A membrane fusion strategy for single-channel recordings of membranes usually non-accessible to patch-clamp pipette electrodes.,” *FEBS letters*, vol. 224, no. 1, pp. 172-6, Nov. 1987.

[20] M. Karlsson, K. Sott, A.-S. Cans, A. Karlsson, R. Karlsson, and O. Orwar, “Micropipet-Assisted Formation of Microscopic Networks of Unilamellar Lipid Bilayer Nanotubes and Containers,” *Langmuir*, vol. 17, no. 22, pp. 6754-6758, Oct. 2001.

[21] T. Lobovkina, I. Gözen, Y. Erkan, J. Olofsson, S. G. Weber, and O. Orwar, “Protrusive growth and periodic contractile motion in surface-adhered vesicles induced by Ca2+-gradients,” *Soft Matter*, vol. 6, no. 2, p. 268, 2010.

[22] N. Düzgünes, J. Wilschut, R. Fraley, and D. Papahadjopoulos, “Studies on the mechanism of membrane fusion. Role of head-group composition in calcium- and magnesium-induced fusion of mixed phospholipid vesicles,” *Biochimica et Biophysica Acta (BBA) - Biomembranes*, vol. 642, no. 1, pp. 182-195, Mar. 1981.

[23] T. A. Oleson and N. Sahai, “Oxide-dependent adsorption of a model membrane phospholipid, dipalmitoylphosphatidylcholine: bulk adsorption isotherms.,” *Langmuir : the ACS journal of surfaces and colloids*, vol. 24, no. 9, pp. 4865-73, May 2008.

[24] Y.-H. Kim, M. M. Rahman, Z.-L. Zhang, N. Misawa, R. Tero, and T. Urisu, “Supported lipid bilayer formation by the giant vesicle fusion induced by vesicle–surface electrostatic attractive interaction,” *Chemical Physics Letters*, vol. 420, no. 4–6, pp. 569-573, Mar. 2006.

[25] R. Tero, T. Urisu, H. Okawara, and K. Nagayama, “Deposition of lipid bilayers on OH-density-controlled silicon dioxide surfaces,” *Journal of Vacuum Science & Technology A: Vacuum, Surfaces, and Films*, vol. 23, no. 4, p. 751, 2005.

[26] I. Gözen, P. Dommersnes, I. Czolkos, A. Jesorka, T. Lobovkina, and O. Orwar, “Fractal avalanche ruptures in biological membranes.,” *Nature materials*, vol. 9, no. 11, pp. 908-12, Nov. 2010.

[27] J. Raedler, H. Strey, and E. Sackmann, “Phenomenology and Kinetics of Lipid Bilayer Spreading on Hydrophilic Surfaces,” *Langmuir*, vol. 11, no. 11, pp. 4539-4548, Nov. 1995.

[28] M. Karlsson et al., “Electroinjection of colloid particles and biopolymers into single unilamellar liposomes and cells for bioanalytical applications.,” *Analytical chemistry*, vol. 72, no. 23, pp. 5857-62, Dec. 2000.

[29] G. Gregoriadis, N. Garcon, H. da Silva, and B. Sternberg, “Coupling of ligands to liposomes independently of solute entrapment: observations on the formed vesicles,” *Biochimica et Biophysica Acta (BBA) - Biomembranes*, vol. 1147, no. 2, pp. 185-193, Apr. 1993.

[30] E. Reimhult, M. Zäch, F. Höök, and B. Kasemo, “A multitechnique study of liposome adsorption on Au and lipid bilayer formation on SiO2.,” *Langmuir : the ACS journal of surfaces and colloids*, vol. 22, no. 7, pp. 3313-9, Mar. 2006.

[31] E. Reimhult, B. Kasemo, and F. Höök, “Rupture pathway of phosphatidylcholine liposomes on silicon dioxide.,” *International journal of molecular sciences*, vol. 10, no. 4, pp. 1683-96, Apr. 2009.

[32] K. Dimitrievski and B. Kasemo, “Influence of lipid vesicle composition and surface charge density on vesicle adsorption events: a kinetic phase diagram.,” *Langmuir : the ACS journal of surfaces and colloids*, vol. 25, no. 16, pp. 8865-9, Aug. 2009.

[33] S. Gromelski, A. M. Saraiva, R. Krastev, and G. Brezesinski, “The formation of lipid bilayers on surfaces.,” *Colloids and surfaces. B, Biointerfaces*, vol. 74, no. 2, pp. 477-83, Dec. 2009.

[34] J. Nissen, S. Gritsch, G. Wiegand, and J. O. Rädler, “Wetting of phospholipid membranes on hydrophilic surfaces - Concepts towards self-healing membranes,” *The European Physical Journal B*, vol. 10, no. 2, pp. 335-344, Aug. 1999.

[35] H. Nabika, A. Fukasawa, and K. Murakoshi, “Control of the structure of self-spreading lipid membrane by changing electrolyte concentration.,” *Langmuir : the ACS journal of surfaces and colloids*, vol. 22, no. 26, pp. 10927-31, Dec. 2006.

[36] I. Gözen, B. Ortmen, I. Põldsalu, P. Dommersnes, O. Orwar, and A. Jesorka, “Repair of large area pores in solid supported double bilayers,” *Unpublished material*, 2012.

[37] D. C. Harris, *Quantitative chemical analysis*, 7th ed. 2007, pp. 378-401.

[38] M. Müller, *Introduction to Confocal Fluorescence Microscopy, Second Edition*. 1000 20th Street, Bellingham, WA 98227-0010 USA: SPIE, 2005.

[39] S. Nie, “Probing Single Molecules and Single Nanoparticles by Surface-Enhanced Raman Scattering,” *Science*, vol. 275, no. 5303, pp. 1018-1021, Feb. 1997.

[40] K. Bacia and J. Schweizer, “Practical Course : Giant Unilamellar Vesicles,” no. September, pp. 1-18, 2005.